POLITECNICO DI TORINO
Repository ISTITUZIONALE

Modelling infrastructure interdependencies and cascading effects using temporal networks

(Article begins on next page)

14 July 2024
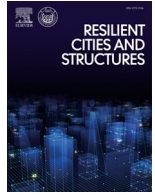
Full Length Article

Modelling infrastructure interdependencies and cascading effects using temporal networks

Gian Paolo Cimellaro [a,*], Alessandro Cardoni [a], Andrei Reinhorn [b]

[a] *Department of Structural, Geotechnical and Building Engineering, Politecnico di Torino, Corso Duca degli Abruzzi 24, 10129, Turin, Italy*
[b] *Department of Civil, Structural and Environmental Engineering, University at Buffalo (SUNY), 135 Ketter Hall, Buffalo NY 14260, United States*

ARTICLE INFO

ABSTRACT

Lifelines are critical infrastructure systems characterized by a high level of interdependency that can lead to cascading failures after any disaster. Many approaches can be used to analyze infrastructural interdependencies, but they are usually not able to describe the sequence of events during emergencies. Therefore, interdependencies need to be modeled also taking into account the time effects. The methodology proposed in this paper is based on a modified version of the Input-output Inoperability Model and returns the probabilities of failure for each node of the system. Lifelines are modeled using graph theory, while perturbations, representing a natural or man-made disaster, are applied to the elements of the network following predetermined rules. The cascading effects among interdependent networks have been simulated using a spatial multilayer approach, while the use of an adjacency tensor allows to consider the temporal dimension and its effects. The method has been tested on a case study based on the 2011 Fukushima Dai-ichi nuclear disaster. Different configurations of the system have been analyzed and their probability of occurrence evaluated. Two models of the nuclear power plant have been developed to evaluate how different spatial scales and levels of detail affect the results.

1. Introduction

Infrastructure systems play an important role in the life of every community. Some infrastructures are so important to social and economic growth and public security that they are called "lifelines". Therefore, this topic has been attracting the attention of researchers who identify lifelines as one of the most important systems to intervene on in order to improve resilience. From the civil engineering point of view, lifelines can be grouped into many categories. Some of the most common networks are power, gas, telecommunication, transportation, water supply, etc. Depending on the demand and the way they are built, critical infrastructures can be extremely interdependent. For instance, Poljanšek et al. [1] studied the seismic vulnerability of the European gas and power networks where the interdependency was evaluated using the level of coupling of the interconnections with the seismic response. The connections among different networks increase the probability of cascading failures and the risk of a tremendous amplification of the consequences. For this reason, it is essential to consider them in risk analysis and resilience assessment [2,3]. Many authors have provided different classifications of various types of interdependencies (Table 1). One of the earliest definition is the one given by Rinaldi et al. [4], which is still a widely accepted classification.

Interdependencies can be mainly categorized into five groups of models: system dynamics-based, network-based, empirical, agent-based, and economic-based. A description of these types of models with their advantages and disadvantages can be found in Cimellaro's book [9] and in Ouyang's work [10]. As pointed out by Sharma et al. [11] though, existing classifications of interdependencies can be biased and inconsistent with the necessary mathematical models. Research on the definition and quantification of system interdependencies is still crucially needed according to Haggag et al. [12]. A novel approach that can be applied following the high level architecture standards to model interdependencies and cascading effects was proposed by Wang et al. [13]. On the other hand, Bayesian networks have been popularly applied for detailed interdependency modeling accounting for uncertainties [14]. However, the computational effort required by Bayesian methods can grow vastly with the number of system nodes.

Researchers have tried to overcome the limitations of older models, especially introducing time as a variable. Time can affect both the topology of the lifelines and the interdependencies among them as failure propagates. Time-dependent analyses are required when temporal inhomogeneity matters and understanding the sequence of the events is crucial. This is usually the case during the emergency response phase where response time should be as short as possible and a number of cascading events might occur [15]. For instance, damages

* Corresponding author.
E-mail address: gianpaolo.cimellaro@polito.it (G.P. Cimellaro).

Table 1
Types of interdependencies according to different authors.

Authors	Types of interdependencies
Rinaldi et al. [4]	Physical, Cyber, Geographic, Logical
Zimmerman [5]	Functional, Spatial
Dudenhoeffer et al. [6]	Physical, Geospatial, Policy, Informational
Wallace et al. [7]	Input, Mutual, Shared, Exclusive, Co-located
Zhang and Peeta [8]	Functional, Physical, Budgetary, Market and Economic

to the power system and debris on roads could compromise communication and water supply systems [16]. Similarly, drainage systems can fail under heavy rainfall events, which cause street flooding leading to an interruption of all services dependent on the use of the road transportation network [17]. Nan and Sansavini [18] studied the impact of interdependencies among infrastructure systems using a hybrid multi-layer approach that captures the dynamics during post-disaster phases. They tested their method on a power supply network consisting of three interdependent subsystems and they highlighted the influence of repair time and delays in the response. Goldbeck et al. [19] proposed a dynamic model consisting of networks and assets representing the components needed to provide services. They then used an algorithm to generate a scenario tree that updates dependencies and active configurations.

This paper proposes a new method derived by the Input-output Inoperability Method (IIM), which belongs to the category of the economy-based models [20]. Given their versatility, input-output methods have been used for many years to investigate the impact of failures and disasters [21] and are still relevant to this day [12]. They can be applied as a tool in resilience assessment at the component level [22] as well as at multi-regional scales for different systems and hazards [23,24]. However, the classic IIM is a static model, so it is not able to manage dynamic dependencies. Many authors have overcome this limitation with

some improvements [25-27]. Different adaptations of IIMs have proved effective to study different types of network systems and their interdependencies. In this study, it has been modified using the approach of temporal networks. In the literature, there are several studies about temporal networks, which are summarized in the research of Holme and Saramaki [28]. This topic is interdisciplinary and here it is applied to interdependent critical infrastructures modeled using graph theory and a spatial multilayer approach. Graph theory has been used for decades to model civil infrastructures. As highlighted in a recent work by Sun et al. [29], it allows modeling rigorously the topology, interdependencies, cascading failures, assigning failure probabilities, and quantifying uncertainties.

The Fukushima Daiichi nuclear disaster has been used as a case study to test the proposed methodology on different scales, as nuclear power plants rely on complex and interdependent infrastructures at both local and regional scales. Nuclear power plants, are characterized by predetermined and accurate emergency and management plans [30]. Thus, risk management is crucial to guarantee safety and prevent disasters. Probabilistic safety analysis (PSA) has been widely used over the last two decades to develop risk monitor tools [31]. Such tools are commonly used to define high-risk configurations due to inactivity or failure of the plant's components, so that proper actions can be taken by operators [32]. The 2011 Fukushima disaster has highlighted the importance of upgrading the equipment to more modern designs and possibly shown the need for additional systems to provide reliable cooling and mitigation strategies for beyond-design events [33]. For instance, Gjorgiev et al. [34] proposed an independent water storage system and used PSA to assess risk. In their model, failure propagation is described through multiple event trees that capture all possible configurations.

In the Fukushima case study, analyzed in Section 4, the focus is not on the nuclear power plant itself, but on the failure propagation through its components, which are supplied by water and power systems. Different configurations of the system in the 24 h after the disruptive events
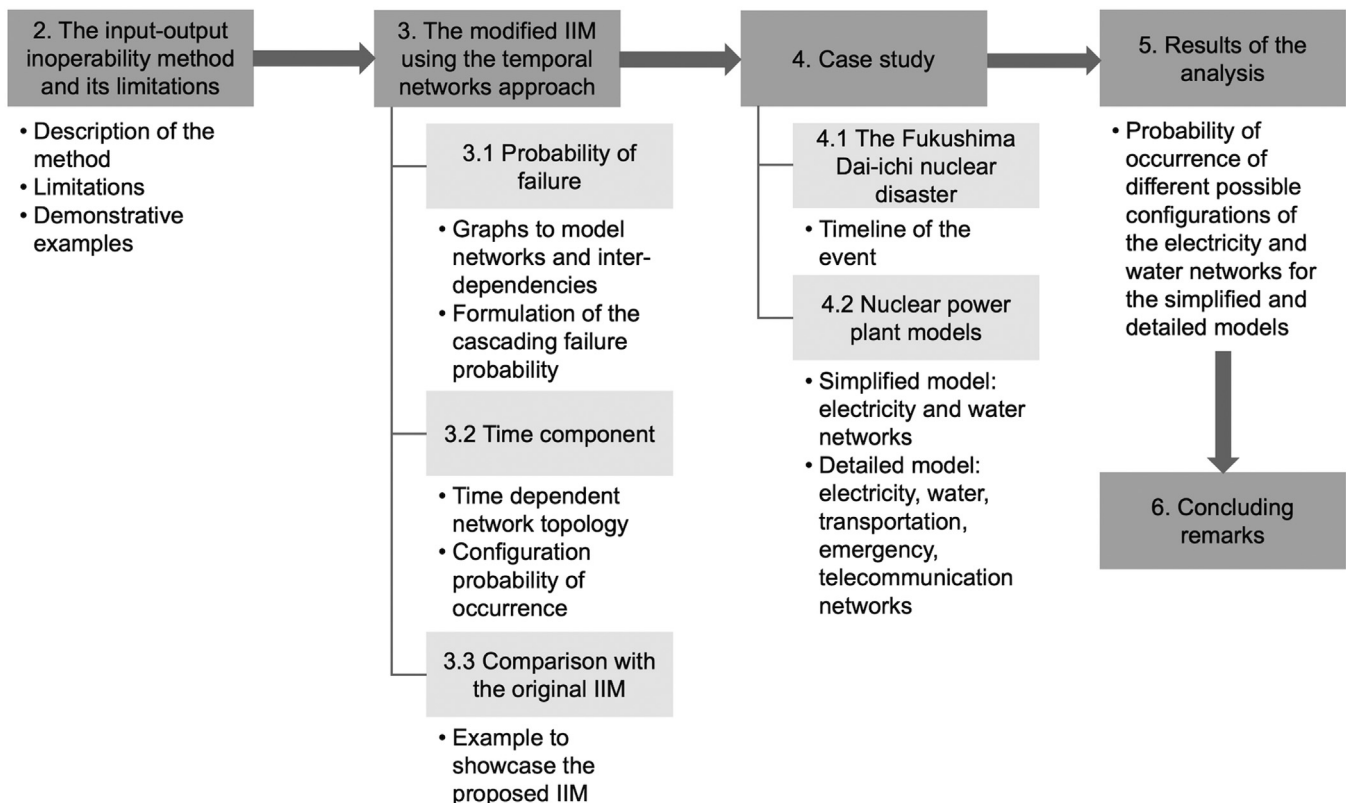
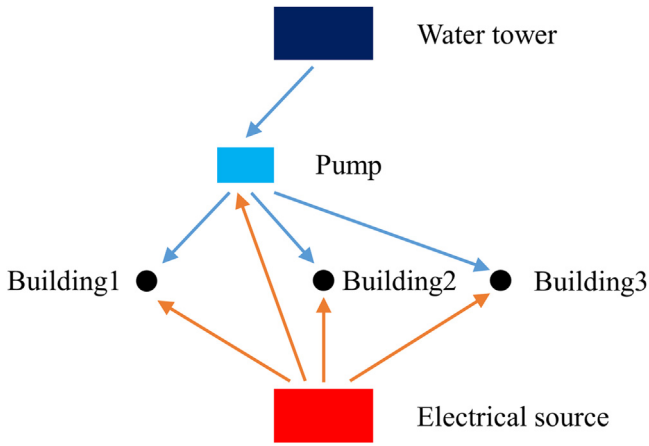**Fig. 1.** Flowchart of the paper structure.

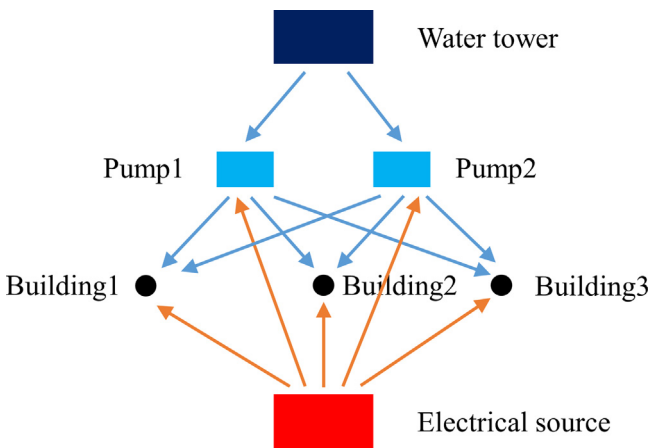**Fig. 2.** Graph representing the topology of Example 1.

Fig. 3. Graph representing the topology of Example 2.

were examined and assigned with a probability of occurrence also considering the interdependencies among involved networks. The proposed IIM was applied to a simplified and a more detailed model of the water and power infrastructure to test the performance of the method on different scales and when different levels of information are available. The flowchart in Fig. 1 summarizes the structure of the following sections of the paper.
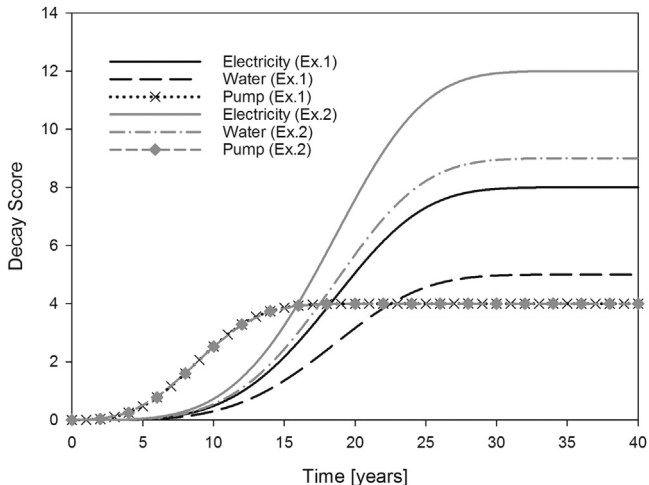

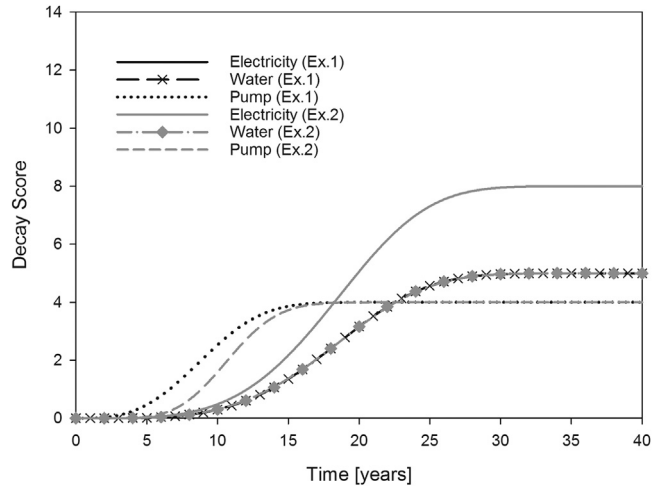**Fig. 4.** Decay scores of Example 1 and Example 2.

Fig. 5. Decay scores of Example 1 and Example 2 considering the effects of redundancies.

2. The input-output inoperability method and its limitations

Critical infrastructures are designed to be reliable even during serious emergencies. Redundancy is a common strategy to increase robustness and therefore backup systems are the best practice. However, to consider the temporal effects, it is required to have a model capable of representing the real configuration of the system at every time step of the analysis.

The new methodology proposed in this paper consists of an improvement of the Input-output Inoperability Method presented by Valencia et al. [35]. The original IIM was developed by Haimes et al. [20] and comes from the Leontief's input-output (I-O) analysis of economic interdependencies [36]. Instead of dealing with economical aspects, the IIM is here intended to simulate the propagation of inoperability among infrastructures. Inoperability is defined by the authors as "the inability for a system to perform its intended function". Mathematically, it is quantified by a value between 0 and 1: when the inoperability of an element is 0, it means that it is working at full capacity, when it is 1, it is completely inoperative. Eq. (1) describes the IIM modified by Valencia et al. [35]:

$$q_i(t) = [I - A]^{-1} c_i(t) \qquad (1)$$

where $q_i(t)$ is the damage vector assessing the inoperability for the node i at the time t; I is the identity matrix; A is the interdependency that describes the connections of the system and corresponds to the adjacency matrix transposed; $c_i(t)$ is the scenario vector which includes the effects of the perturbation (e.g. natural disasters, terroristic attacks, intrinsic
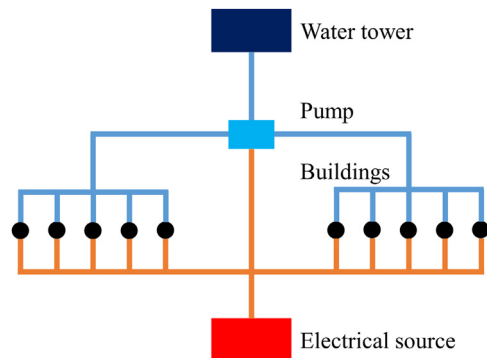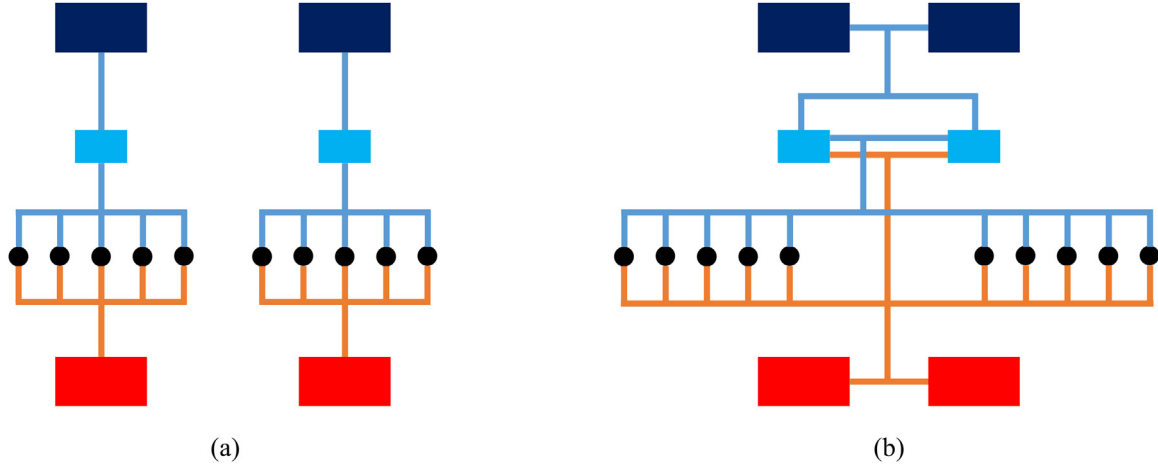

Fig. 6. Topology of Example 3.

(a)   (b)

Fig. 7. (a) Spin-off and (b) redundancy interventions applied to the system of Example 3.

failures, etc.) on the node i at the time t. The damage vector is the output of the model and quantifies the inoperability level of the system's infrastructures after the propagation of an event according to the interdependency matrix (A). Each element of A expresses the influence of the jth infrastructure on the ith infrastructure. Values can be either 1 (complete propagation of the scenario from j to i) or 0 (no propagation from j to i). Considering the infrastructure aging as a hazard, the sum of the elements of the damage vector q of each node i at each time t represents the impact that a single node has on the network. This index is referred to as decay score (Eq. (2)). A large value of the dc_s means a high impact of component i to the remaining part of the network.

$$dc\_s_i(t) = \sum_{i=1}^{j} q_i(t) \tag{2}$$

This approach, although effective to extend the original method, presents some limitations when applied to complex infrastructure networks. Firstly, it does not consider the redundancies of the system. Secondly, it may be difficult to properly consider the evolution of the entire system over time and to evaluate the probability that each node will fail.

A simple improvement is suggested to overcome the limitation related to redundancies. As an example, the six-node network developed by Valencia et al. [35] is considered and referred to as Example 1. It illustrates the system consisting of electricity and water distribution networks serving three buildings (Fig. 2). To assess the effect of redundancies, another pump station is introduced. Fig. 3 shows the new topology of the system (Example 2).

Obviously, the performances are improved compared to the previous situation since two pumps are doing the same work. Thus, if a pump fails, the other one can meet the demand, assuming that simultaneous failure is not possible. Given that, it is reasonable that the decay scores of the water tower and the electrical source remain the same, while the decay score of the pump houses should decrease. Nevertheless, comparing the obtained results, it is possible to see how the expected trends are not met using the IIM proposed by Valencia et al. [35] (Fig. 4). The dc_s of the electrical source and the water tower increase, while pumps' decay score does not change. However, this result is still not adequate as the algorithm considers the second pump as another node to be fed by them. To avoid this, the Series-Parallel vector (SP) is introduced in Eq. (3):

$$SP = \begin{Bmatrix} 1/n_1 \\ 1/n_2 \\ \vdots \\ 1 \end{Bmatrix} \tag{3}$$

where n_i represents the number of redundancies for the node i. Extending the SP vector to the n-dimension (Eq. (4)) it is possible to modify

the equation of the damage vector as shown in Eq. (5):

$$SP^* = SP \times \begin{Bmatrix} 1 & 1 & \cdots & 1 \end{Bmatrix}_{1 \times n} \tag{4}$$

$$q_i(t) = \left[I - A \cdot SP^* \right]^{-1} \cdot c_i(t) \tag{5}$$

After this modification, the results of the model fulfill the initial expectations about redundancy effects, as shown in Fig. 5.

To represent the performance of the entire system, it is possible to introduce another index based on the decay score, namely the system status (s_s). This dimensionless positive index is meant to assign a scoring to a system of infrastructures at a specific time t and it is defined by Eq. (6):

$$s\_s(t) = \sum_k \frac{\sum_i dc\_s_{k,i}(t)}{n_k} \tag{6}$$

where k is the category of nodes (e.g. electrical sources, water towers, pump houses, etc.) and i is the corresponding node. A small value of the s_s denotes that the system of infrastructures has a low risk of critical nodes' failure, while a large value indicates high risk. The threshold dividing the low-risk area from the high-risk one needs to be calibrated according to the importance of the system and the minimum acceptable performance. Through this index, a sensitivity analysis can be performed to evaluate the advantages of the different interventions on the topology of the system. For instance, let us consider Example 3 in Fig. 6. Two potential interventions to increase the performances could be the spin-off
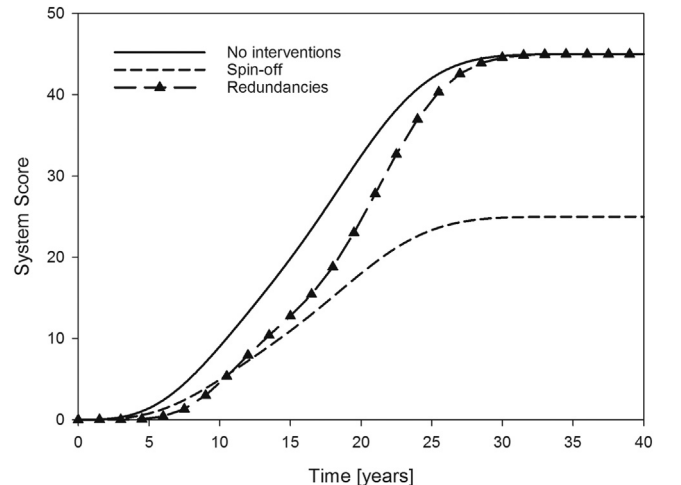

Fig. 8. Decay scores of Example 1 and Example 2.

Network perturbation

Fragility curves

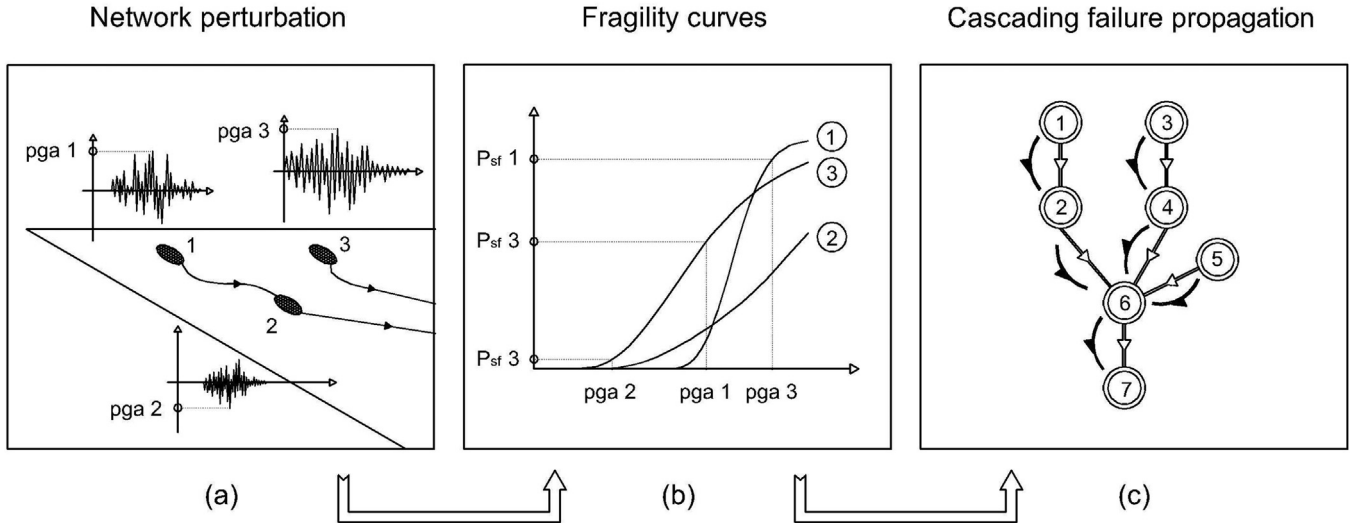## Cascading failure propagation

Fig. 9. Flowchart of the probabilistic approach. After a perturbation of the network (a), the nodes' probabilities of failure are computed using fragility curves (b) and then propagated according to the configurations of the network (c).

and the introduction of redundant components as illustrated in Fig. 7. The results obtained from the calculation of the system status are illustrated in Fig. 8. Looking at the redundancy intervention, it is possible to notice how the s_s significantly decreases in the short term, while after 30 years there are no benefits compared to the original configuration of Example 3. The spin-off turned out to be the best intervention in this situation since the entire curve is lowered and the value of the plateau is almost halved.

3. The modified input-output inoperability model using the temporal networks approach

3.1. Probability of failure

In the modified IIM networks are modeled using graph theory. The topology of a network is represented by a graph $G(N, L)$ that consists of a set N of nodes (or vertices) and a set L of links (or edges). The level of detail of graph components depends on the scale which might be an entire infrastructure (e.g., power, water, gas network), a sub-system

(e.g., wind turbine), or even a single component (e.g., gearbox of a wind turbine). Moreover, specific features can be assigned to each node and edge. In the proposed model, edges are directed. This means that each link can be passed through only in one way. Two cases may occur: edges connecting nodes intra-network, that is within the same infrastructure, or inter-networks, i.e., among different infrastructures. In this model any inter-network link is Boolean. Thus, the value $a_{xi,yj}$ is 1 if the xth node belonging to the ith infrastructure is dependent on the yth node of the jth infrastructure and 0 otherwise.

The concept of "chain" is also introduced in the model. A chain is a sequence of vertices connected by certain edges and it defines an active configuration. Sources are the starting point of a chain. These are nodes without inflow edges. The other nodes have only one inflow edge at a time and one or multiple outflow edges. If backup systems are present, in case of failure of the primary source, the inflow edge is replaced with another one coming from a different upstream source. Different configurations ensure better reliability of the network, though they can be active one at a time. The design of the infrastructure itself defines the hierarchy of activation. If some components of the main chain fail, an al-
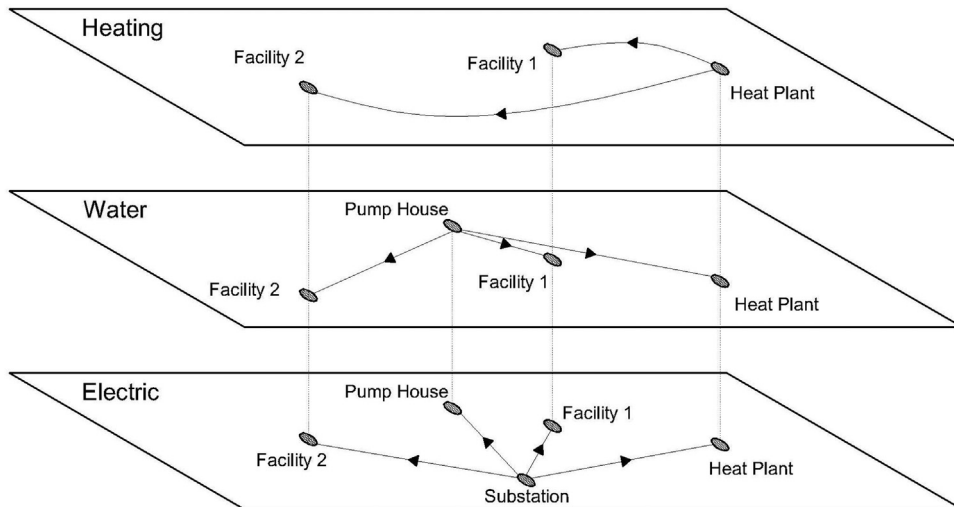

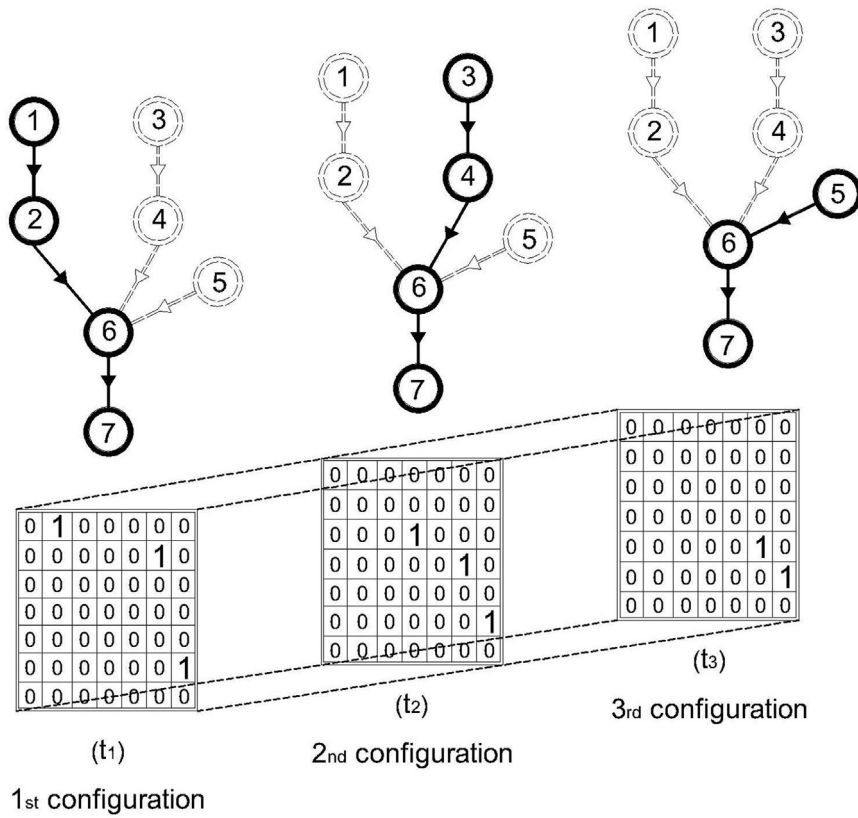**Fig. 10.** Multilayer representation of interdependent networks.

Fig. 11. Example of a tensor showing three possible and mutually exclusive configurations of a network described by different adjacency matrices.
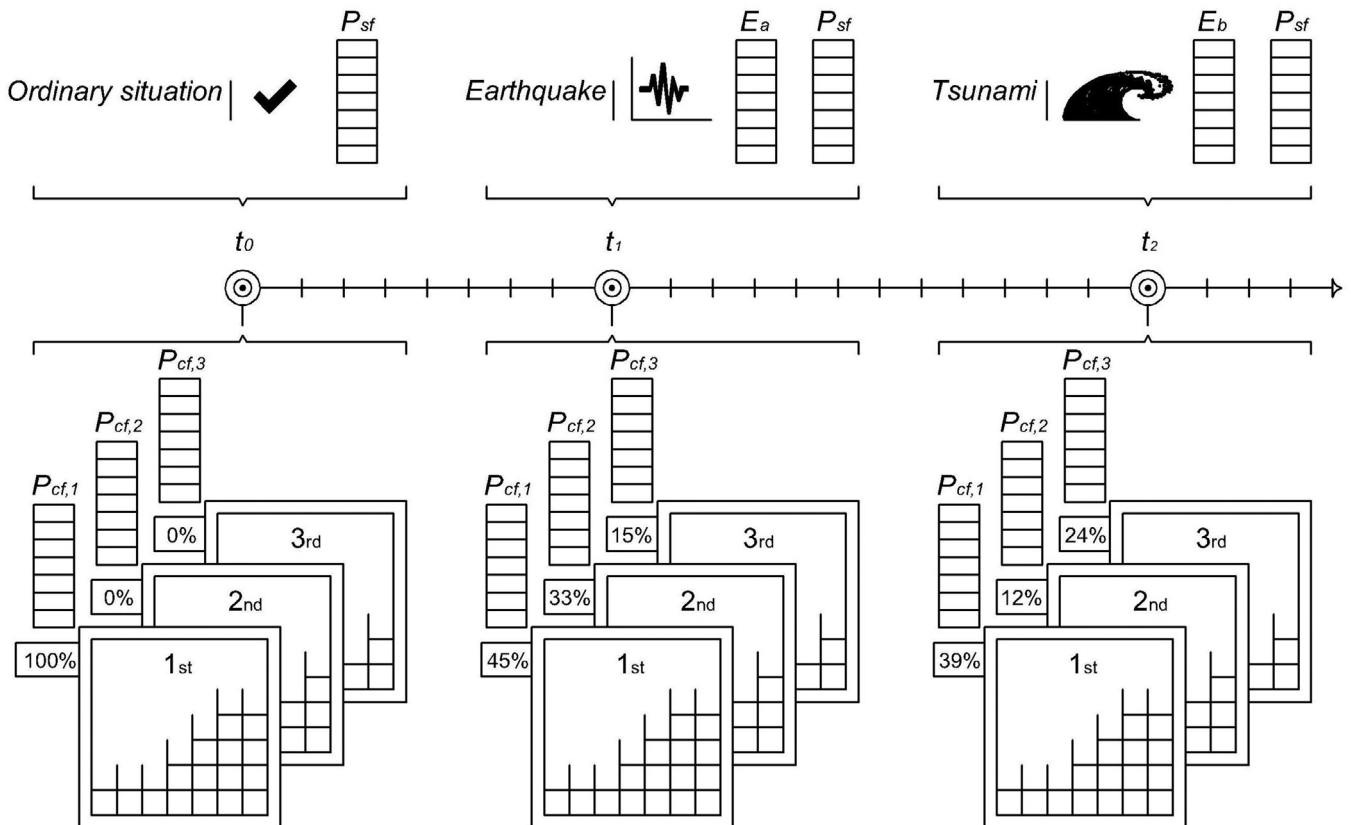

Fig. 12. Variation over time of the probability of occurrence for different configurations following disruptive events.

ternative chain originating from the same source activates. When there are no more alternatives, backup sources come into operation and new chains are defined.

As seen in Section 2, the decay score gives an idea of the cascading propagation of inoperability, but it is not able to evaluate the status of the nodes. Therefore, a probabilistic approach has been used in the modified IIM. In detail, a failure probability is assigned to each node by combining the hazard magnitude with the infrastructure's vulnerability and related to the status of the node itself after the perturbation (i.e., fully functional or failed). The hazard component is represented by an event vector E ($n \times 1$), where n is equal to the number of the system's nodes. The elements of the E-vector are quantities such as peak ground acceleration (pga), peak ground velocity (pgv), peak ground displacement (pgd), the wave height (Wh) of a tsunami, the megatons (Mt) of an explosion, etc. The values of these quantities may vary from one node to another, as infrastructures usually have a large spatial extension (Fig. 9a). The probability that the considered event might occur with a given magnitude is obtained from the hazard curves. The vulnerability of each component is instead evaluated through fragility curves (Fig. 9b). Only the fragility curves related to complete failure have been used, while other damage states are not considered in this paper.

The total probability of failure (P_f) of each node in the system is obtained as a combination of the self-failure probability (P_{sf}) and the cascading failure probability (P^*_{cf}). The two events are not disjoint and therefore P_f is given by the following equation:

$$P_f = P_{sf} + P^*_{cf} - P_{sf} \cdot P^*_{cf} \tag{7}$$

The cascading failure probability (P^*_{cf}) depends on the actual configuration of the system (Fig. 9c), and for the ith network it is given by Eq. (8):

$$P^*_{cf,i} = \left(Y^T_{j \leftrightarrow i} \cdot P_{cf,j} \right) + P_{cf,i} - \left(Y^T_{j \leftrightarrow i} \cdot P_{cf,j} \right) \cdot P_{cf,i} \tag{8}$$

where $P_{cf,i}$ is the cascading failure probability vector, whose elements are obtained by combining the self-failure probability of a given node and the one of the upstream node within the same network (Eq. (9)); $P_{cf,j}$ is the cascading failure probability vector of the jth interdependent network; $Y_{j \leftrightarrow i}$ is an adjacency matrix which indicates interdependent nodes between networks i and j. This is a rectangular $n \times m$ matrix, where n is the number of nodes of network i and m is the number of nodes of infrastructure j.

$$P_{cf,i(k)} = P_{sf,i(k)} + P_{sf,i(k-1)} - P_{sf,i(k)} \cdot P_{sf,i(k-1)} \quad k = 2, ..., n \tag{9}$$

For visualization purposes, different infrastructures can be seen as separate layers and virtually connected to represent interdependence. Nodes that are dependent on multiple networks are projected on the corresponding layers (Fig. 10). The advantage of this approach is that infrastructure managers can perform the analysis on their infrastructure of competence to identify critical nodes while monitoring possible effects on other layers. Moreover, it can be easily integrated with geographic information system (GIS) platforms which also adopt a layer structure.

3.2. Time component

The main step forward compared to the traditional static IIM is the introduction of a timeline $\tau=[t_0, t_1, t_2, ..., T]$, where the range $t_0 \div T$ must be extended enough to include all the disruptive events and their consequences. Each time step Δt of the τ vector represents the time necessary for the propagation of the event over the entire system. This means that if at the time t' a landslide destroys a transmission tower, at the time $t'+\Delta t$ a new configuration of the system will be active. Therefore, the temporal networks' approach is introduced. Each network can be described with a time-dependent graph, denoted as $G(t) = G(V, L(t))$. This implies that chains are generated not only by spatial layers but also
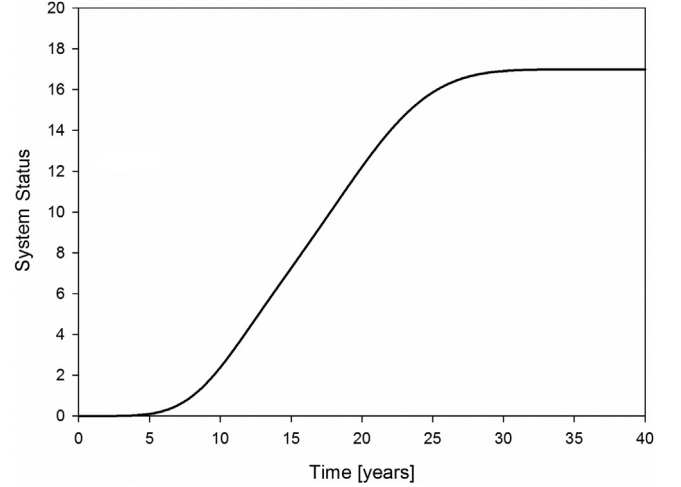

Fig. 13. System status of Example 2 according to the IIM.

by different temporal layers. The adopted strategy consists in updating the two-dimensional matrices defining spatial configurations with a three-dimensional tensor notation. The topology of each network is now described by an adjacency tensor, whose elements are $a(t)_{xi,yj}$. Different temporal layers of the adjacency tensor represent possible chains that activate following a given hierarchical rule. Fig. 11 shows three different possible configurations of a seven-node network.

To better understand which chain is active at a given time, the probability of occurrence of a specific configuration P_{occ} is assigned to every layer (Fig. 12). This variable indicates if the layer is active ($P_{occ} = 1$), or not ($P_{occ} = 0$) at the considered time step of the analysis. The sum of the probabilities of occurrence is $0 \leq \Sigma P_{occ} \leq 1$ and the value $1 - \Sigma P_{occ}$ represents the loss of capacity of the network (LoC). It is worth noting that some layers corresponding to backup configurations can stay active only for a limited period of time as backup sources may have limited autonomy. This is the case, for example, of diesel generators whose autonomy depends on the capacity of the diesel tank.

3.3. Comparison with the original IIM

A comparison between the results obtained from the modified IIM and the original IIM proposed by Valencia et al. [35] was carried out to evaluate the improvements of the method. Example 2 was used as a

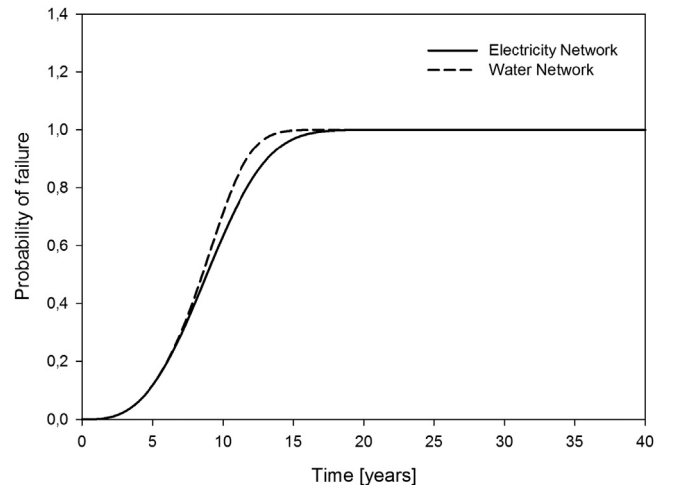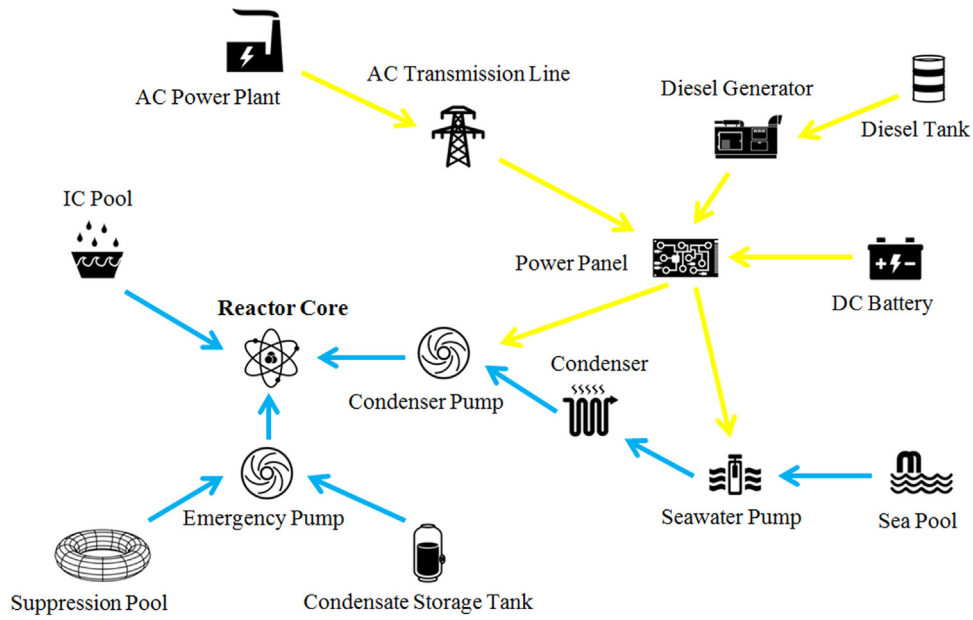**Fig. 14.** Networks' failure probability of Example 2 according to the modified IIM.

Fig. 15. Simplified model of the electricity and water network serving the nuclear power plant.
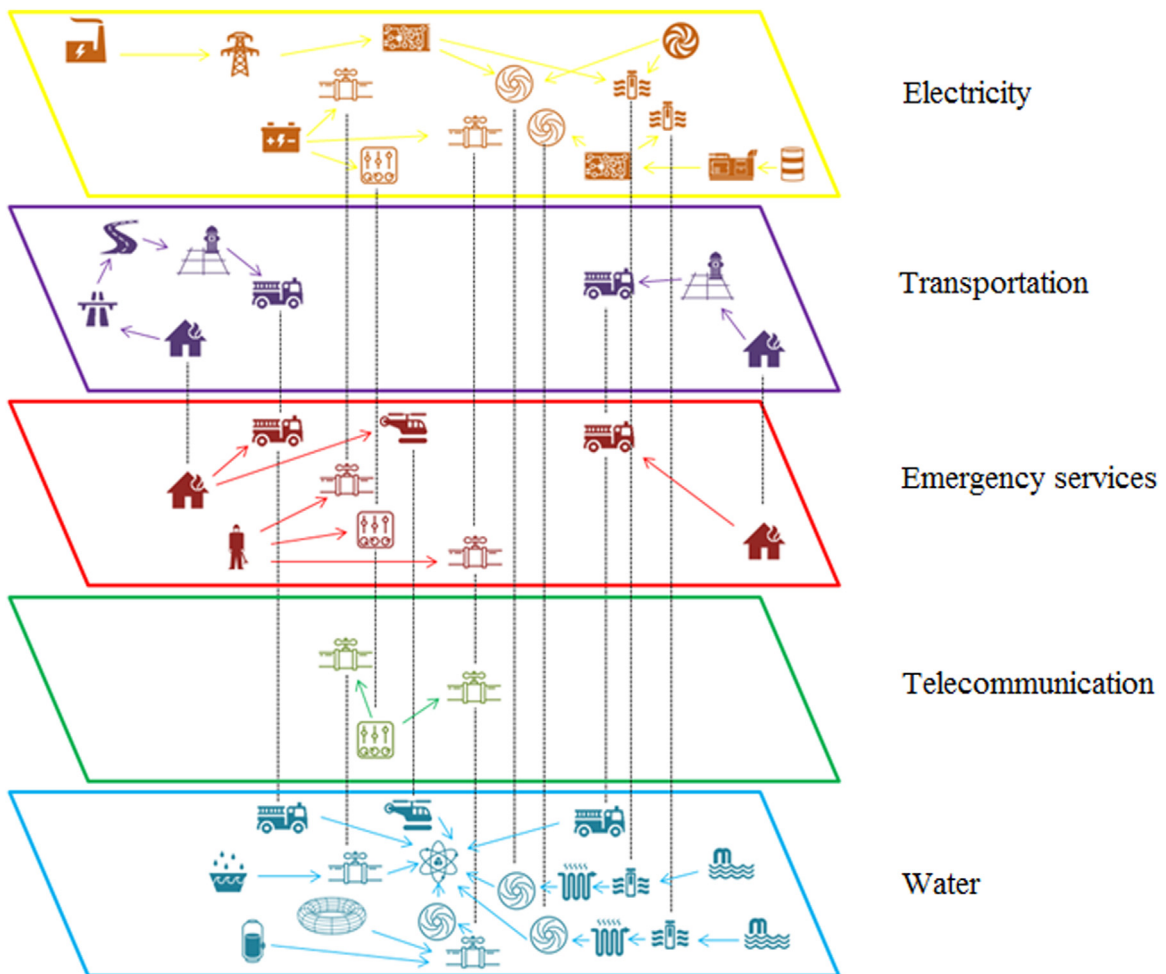

Fig. 16. Interdependent lifelines of the detailed model.

testbed for this comparison. To evaluate the overall performance of the system, the system status s_s was introduced and defined as the sum of the elements of the q-vector. Its limitation is that it does not give information about the components' status and a threshold should be defined to evaluate the actual performance of the system. On the other hand, the modified IIM is based on probabilities of failure, which provides a more reliable performance measure. Comparing the results, Fig. 13 shows the system status for the power and the water networks using the IIM proposed by Valencia et al., while Fig. 14 illustrates the failure probability for the same networks obtained through the proposed method, considering that a network fails when all its nodes fail. It can be observed that they are inactive ($P_f = 1$) after about 17 years, which cannot be deduced from the s_s curve of Fig. 13.

4. Case study

4.1. The Fukushima Dai-ichi nuclear disaster

The case study is inspired by the Fukushima Dai-ichi nuclear disaster, which is a comprehensive example of failure due to interdependencies and temporal effects. The complexity of the events and the system were not accurately considered by risk planners, so that cascading effects resulted in huge damages to the nuclear power plant. In the 1960s and 1970s, it was common international practice to use historical records when applying methods for estimating the vulnerability to seismic and concomitant hazards. This common practice included increasing safety margins, which, however, was not considered for the design of reactors 1 and 2. The partial retrofitting done in 2009 was still insufficient to withstand the intensity of the 2011 events.

A brief description of the timeline of the events is provided to better understand the following characterization of the model.

The Tohoku earthquake and tsunami that struck Fukushima Dai-ichi nuclear power plant on March 11, 2011, destroyed the backup systems causing the failure of three reactors, fuel melting, hydrogen explosions, and radioactive contamination, which forced about 83,000 people to evacuate. First, the earthquake caused the loss of off-site power supplies, so backup diesel generators turned on as expected. Units 1, 2, and 3 shut down automatically and were able to maintain sufficient cooling. However, the subsequent tsunami flooded the electrical switchgear of the diesel generators, and units 1 to 3 stopped working. Unit 4 was undergoing maintenance, so the nuclear fuel had been removed previously and placed in the unit's spent fuel storage pool. Nonetheless, it caused a considerable release of radioactivity. Only units 5 and 6 continued to be cooled. Since electronic security equipment of units 1, 2, and 3 were unable to work, it was not possible to remove the heat and pressure from the reactor cores. As the fuel overheated, it reacted with steam producing huge quantities of hydrogen. The generated explosions interfered with the efforts done by the workers to restore the cooling system. The radioactive substances released into the atmosphere, produced an extremely high radiation dose rate nearby the plant and left wide uninhabitable areas, especially in the north-west site.

4.2. Nuclear power plant models

To reproduce what happened at Fukushima, it is necessary to have accurate models for all the networks serving the nuclear power plant. This work is not meant to model Fukushima Daiichi NPP exactly since data regarding this case study are not comprehensive, or inaccessible to the authors. Therefore, the topology and the data related to the disrupt-
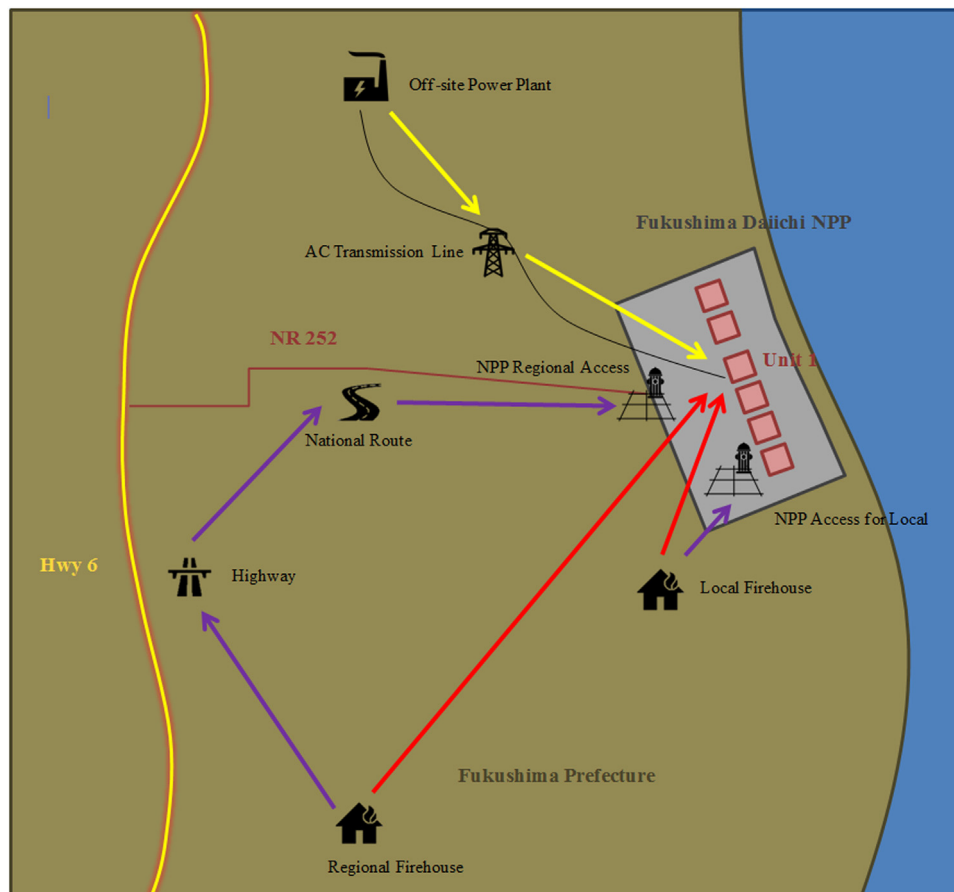

Fig. 17. Detailed model of the considered lifelines at the regional scale.

ing events affecting the system are inspired by the events that occurred on 11th March 2011, while specific parameters of the components are taken from the literature. Nuclear power plants are dependent on several infrastructures. Focusing on the connectivity of these networks, it is possible to define a logical topology of a model. The plant scheme of unit 1 provided by the Tokyo Electric Power Company was used as a guideline to develop the model. In that scheme, there are electricity, water, and steam networks. The latter has not been considered as a separate system, but it has been merged with the water system. Possible configurations have been modeled with directed links from the source to the reactor core. Two different models have been developed, a simplified and a detailed one.

The simplified model is shown in Fig. 15 and it is composed of the electricity and the water network. The water network is a local scale network, whereas the electric network extends from the regional to the local scale. Since the aim is to run a performance analysis of all the systems serving the reactor core, all the fundamental components have been modeled as nodes and connected to each other following specific paths. The sources of the electricity network are, in order of priority: (i) external electric power network, (ii) diesel generators, and (iii) DC batteries. All of them converge into a power panel which then supplies the pumps of the water network whose source is

the sea. The first emergency cooling system is the Isolation Condenser (IC), which can cool down the steam of the reactor and does not need electricity because the flow is gravity driven. In addition, the High-Pressure Coolant Injection system (HPCI) can cool the core in emergency conditions by taking water from the Condensate Storage Tank (CST) or the Suppression Pool (SP). Given the design of Units 1–4, the HPCI does not need electricity as well since the pump is steam driven.

Because of the complexity of both the electricity and the water network, a detailed model has been built based on different assumptions. Firstly, to better model human behavior during the emergency, three additional networks have been considered: the telecommunication, transportation, and emergency service network. Each network is represented by a layer, as shown in Fig. 16. The cross-layer links indicate the interdependencies among different networks. The connections among nodes can be at the regional scale (Fig. 17), at the local scale (Fig. 18) and at the reactor scale (Fig. 19). Each source supplies target nodes. The ordinary cooling system, for instance, is only fed by the off-site electricity network and the NPP turbine, whereas diesel generators supply the Residual Heat Removal (RHR) cooling system through the in-site power panel (Fig. 18). The IC and HPCI systems, which in the simplified model have been considered independent on electricity, are now indirectly de-
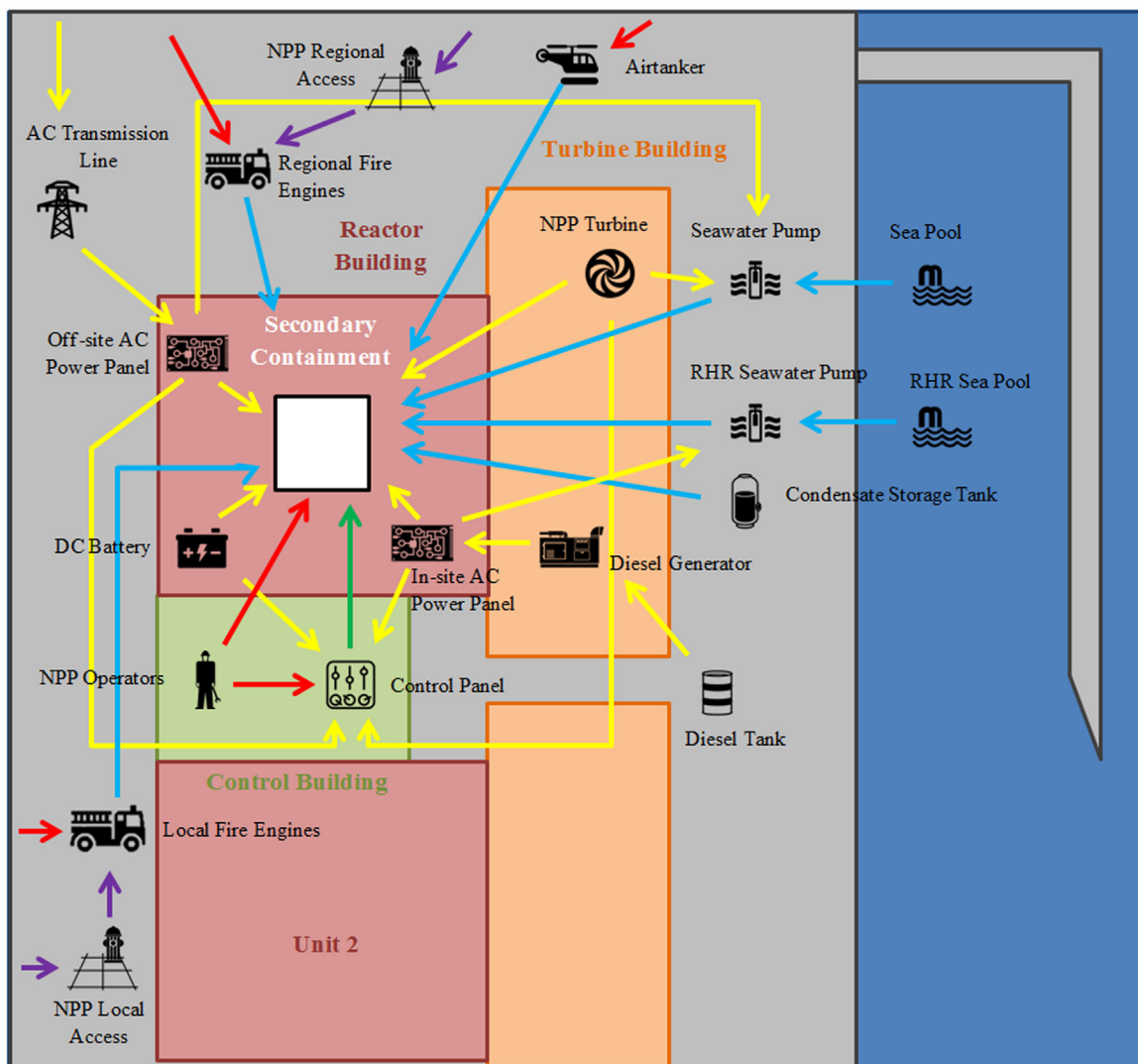

Fig. 18. Detailed model of the considered lifelines at the local scale.
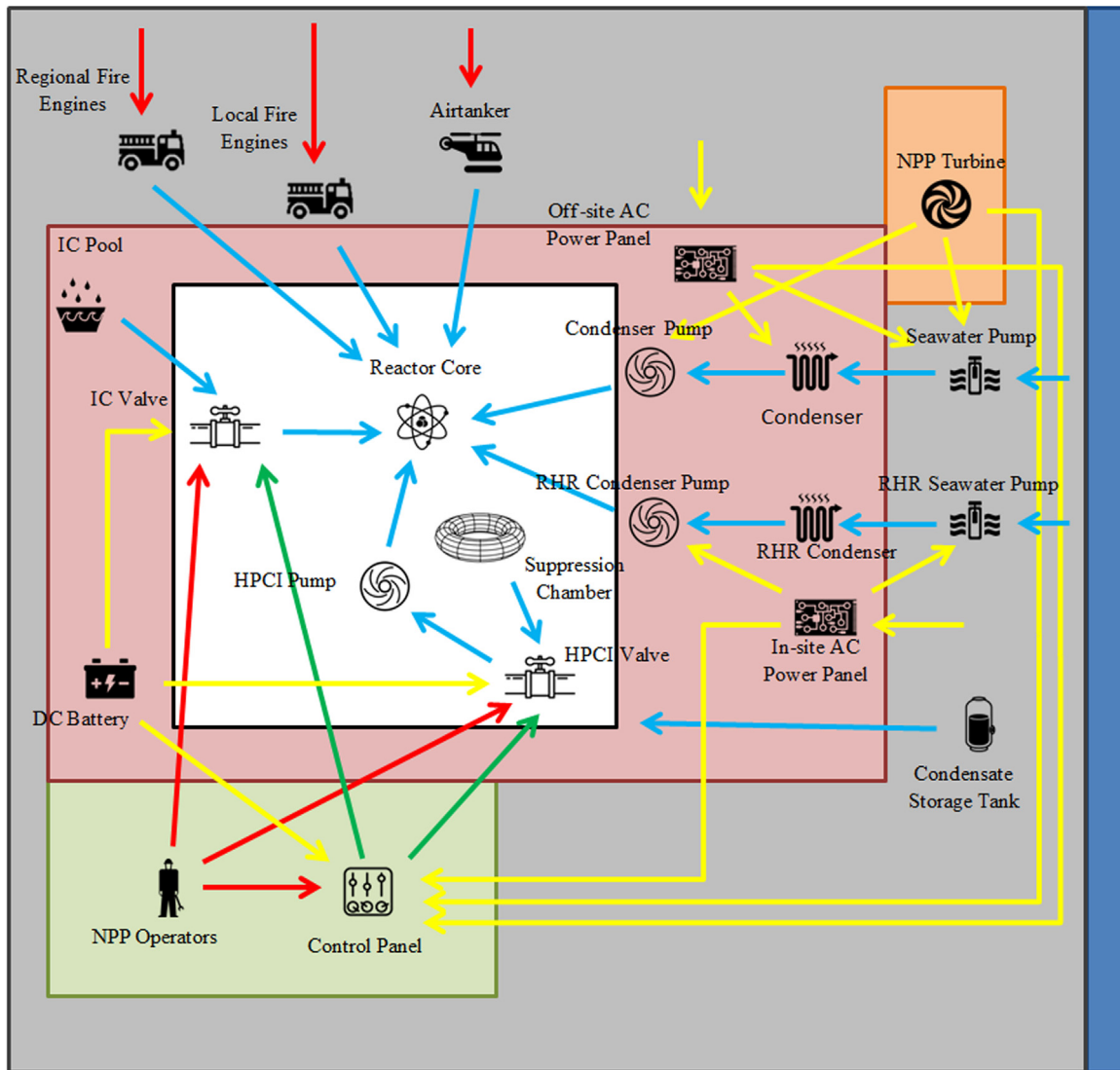
Fig. 19. Detailed model of the considered lifelines at the reactor scale.

pendent on it because their activation is performed by valves which can be remotely controlled only with electricity supply given by the DC battery (Fig. 19).

The magnitude of the two hazards, i.e., earthquake and tsunami, have been evaluated in terms of Peak Ground Acceleration (PGA) and Wave Height. They are deterministic and taken form the records of the real event. Nodes have been classified according to their location so that for each one it is possible to assign the intensity of the event as shown in Table 2.

Time steps of the analysis are defined following the timeline of the events that occurred in Unit 1 of Fukushima Dai-ichi nuclear power plant. In particular, the 24 h following the earthquake have been analyzed with one-hour time steps. Regarding the fragility functions considered in the analysis, most of them are taken from ATC-13 "Earthquake damage evaluation data for California" [37], a data source from the literature that is still broadly used. ATC-13 provides matrices showing the damage probability for some structural and non-structural components. Additionally, both the ALA report [38] and the Hazus database [39] were consulted to get additional earthquake fragility curves. Tsunami fragility curves have been obtained through linear interpolation of the values given by the ATC-13 recommendations. Finally, autonomy curves have been approximated as step functions where each step represents the nominal value reported by Hitachi-GE [40].

5. Results of the analysis

This section shows the results related to the electric and water networks of both the simplified and detailed models of the NPP. The analyses of the other networks included in the detailed model are not reported since they cannot be compared with the simplified model. However, they have been taken into account while performing the analyses. In the simplified model, the earthquake is responsible for the collapse of the AC transmission line; thus, the electric network fails (configuration 1). However, the power supply to water network components is guaranteed by diesel generators (configuration 2). Other components suffer minor or no damages. When the tsunami wave strikes, diesel generators fail, and DC batteries are seriously damaged (configuration 3). However, there is no need for them anymore since the pumps have already failed (Fig. 20).

As far as the water network is concerned, configuration 1 is represented by the seawater pump that stops working when the earthquake strikes. Subsequently, the IC backup cooling system turns on and the probability of failure of the reactor core is still close to 0 (configuration 2). Ten hours after the earthquake, the autonomy of the IC starts decreasing and it is replaced by the HPCI system, which does not need electricity and consists of the condensate storage tank (configuration 3) and the suppression pool (configuration 4). Fig. 21 shows the proba-

Table 2

Intensity of the hazards for the components of the models.

| Node	Location	Altitude [m]	PGA [g]	Wave Height [m]
NPP Turbine	Turbine Building	10	0.469	6
AC Power Plant	Hinterland	>50	0.415	–
AC Line	Hinterland	>50	0.415	–
Off-site AC Power Panel	Turbine Building	10	0.469	6
Diesel Tank	NPP Apron	10	0.469	3
Diesel Generator	Reactor Building	10	0.469	9
In-site AC Power Panel	Reactor Building	10	0.469	9
DC Battery	Reactor Building	10	0.469	9
Highway	Hinterland	>50	0.415	–
Road	Hinterland	>50	0.415	–
Local Firehouse	Hinterland	>50	0.469	–
NPP Local Access	NPP Apron	10	0.469	3
Local Fire Engines	–	–	0.469	–
Regional Firehouses	Hinterland	>50	0.415	–
NPP Regional Access	NPP Apron	10	0.469	3
Regional Fire Engines	–	–	0.415	–
Airtanker	–	–	0.415	–
NPP Operators	–	–	0.469	–
Control Panel	Control Building	10	0.469	6
Sea Pool	Wharf	4	0.469	5
Seawater Pump	Wharf	4	1.000	3
Condenser	Reactor Building	10	0.469	9
Condenser Pump	Reactor Building	10	1.000	9
RHR Sea Pool	Wharf	4	0.469	5
RHR Seawater Pump	Wharf	4	0.469	3
RHR Condenser	Reactor Building	10	0.469	9
RHR Condenser Pump	Reactor Building	10	0.469	9
IC Pool	Reactor Building	10	0.469	9
IC Valve	Reactor Building	10	0.469	9
Condensate Storage Tank	NPP Apron	10	0.469	3
Suppression Pool	Reactor Building	10	0.469	9
HPCI Valve	Reactor Building	10	0.469	9
HPCI Pump	Reactor Building	10	0.469	9
PCV	PCV	20	0.469	16
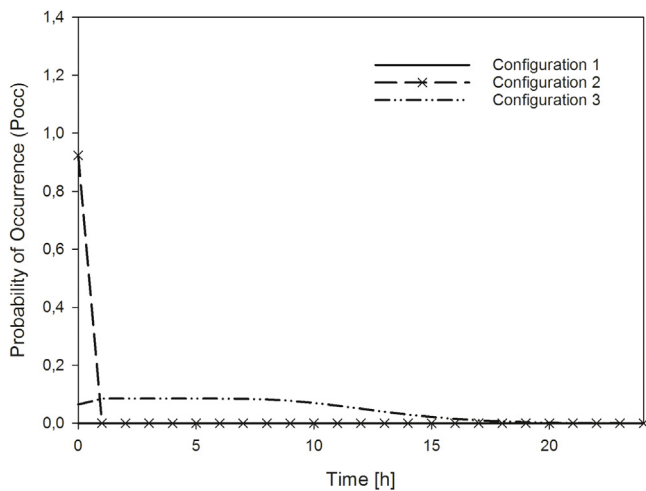
Fig. 20. Probability of occurrence vs time for the power network's different configurations using the simplified model.
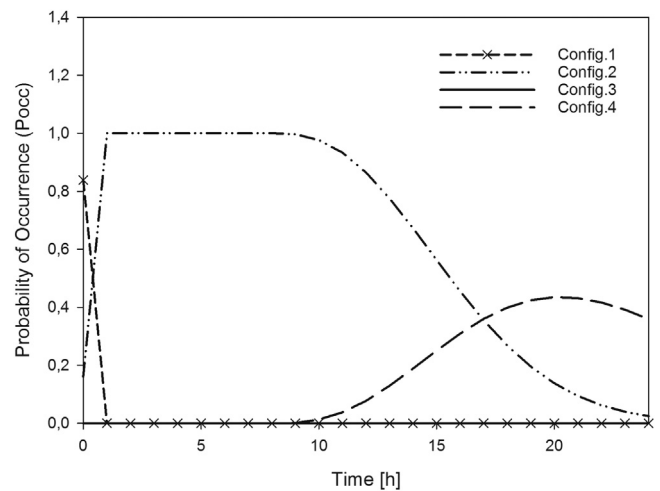

Fig. 21. Probability of occurrence vs time for the water network's different configurations using the simplified model.

bility of occurrence calculated for the four configurations of the water network described above. The HPCI system is seriously damaged by the earthquake and the tsunami. Therefore, the probability of failure of both the IC and reactor core increases rapidly (Fig. 22).

In the detailed model, the earthquake is responsible for the shut-down of the off-site AC power (configuration 1) and the NPP turbine (configuration 2). Electricity is provided by diesel generators (configuration 3) until the arrival of the tsunami waves that damage also the DC batteries (configuration 4). Fig. 23 shows the probability of occurrence of the four configurations of the power network during the emergency.

The damage to the electric network cause negative effects on the water cooling system. In the detailed model eight configurations have been identified:

- configuration 1: seawater pump;
- configuration 2: Residual Heat Removal system;
- configuration 3: IC pool;
- configuration 4: Condensate Storage Tank;
- configuration 5: suppression pool;
- configuration 6: local fire rescue;
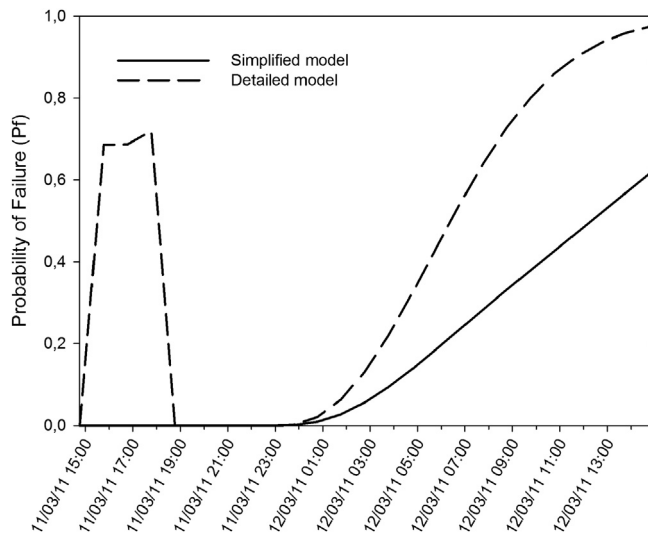- configuration 7: regional fire rescue;

Fig. 22. Probability of failure of the reactor core for the simplified and detailed models.
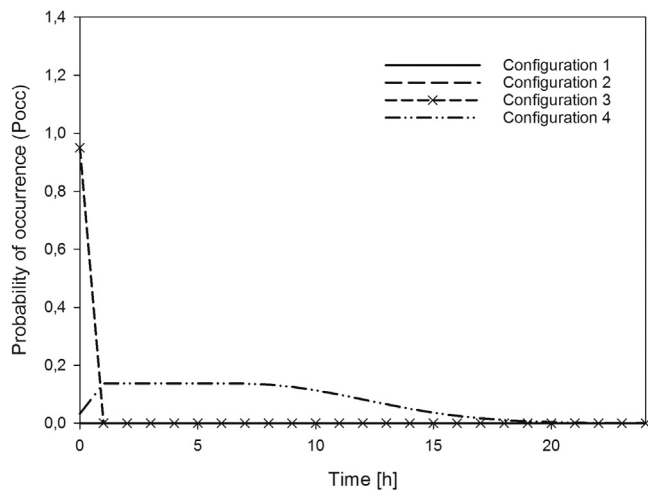

Fig. 23. Probability of occurrence vs time for the power network's different configurations using the detailed model.

- configuration 8: air tanker.

Fig. 24 shows results in terms of probability of occurrence for each configuration. The ordinary seawater pump is the first to fail. Electricity is still provided by diesel generators that supply the Residual Heat Removal system. After the tsunami, the diesel tanks, CST, and RHR seawater pump are completely damaged and the access to the NPP is not usable because of debris brought by the wave. DC batteries are needed to control the IC and the HPCI, but they are damaged. Consequently, the probability of failure of the reactor core sharply increases. After three hours, IC valves are manually activated so the IC cool down the reactor until its autonomy runs out leading to a complete loss of capacity (Fig. 22).

The performed analyses show that both models are successful in depicting the situation for the electric network, while on the other hand there are some differences between the results obtained for the water network. In regard to the power network, there are no large differences as the topology of the two systems differ only by the number of power panels and target nodes' supply lines. Moreover, the electric network is not dependent on any other, thus adding and detailing other networks does not have any influence. In the water network results, there are some discrepancies because in the detailed model many power sources sup-
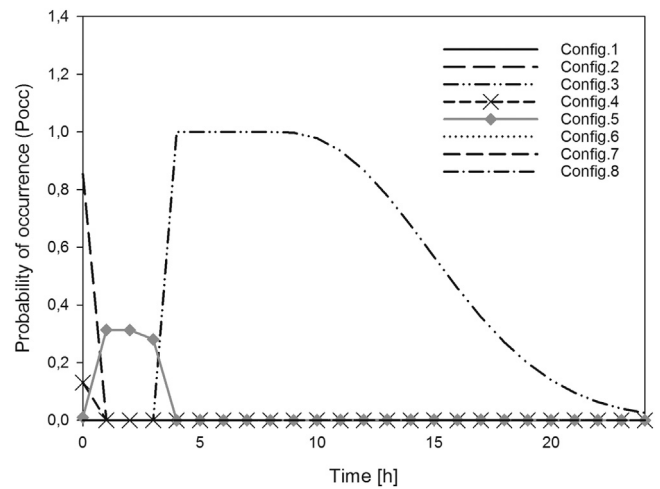

Fig. 24. Probability of occurrence vs time for the water network's different configurations using the detailed model.

ply various components of the water-cooling system. The greater level of interdependency, which characterizes the detailed model, results in a more complex trend of the reactor core's failure probability. Therefore, the detailed model can catch better variations in the configuration of lifelines over time. To improve this aspect, future work needs to be geared towards the selection of more input data.

6. Concluding remarks

In this article, a methodology to model critical infrastructure networks has been proposed. Natural and man-made disasters are likely to cause serious damages to critical infrastructures because of their complexity and interdependence. The first consideration that has been made is that the analysis of a single network's components alone is not enough to reduce vulnerability. Multiple networks should be analyzed simultaneously as cascade effects due to interdependencies are likely to cause disproportionate damages. This work introduces a modified Input-output Inoperability Method (IIM) containing three improvements compared to the traditional one. Firstly, a probabilistic approach is used. Hazards, fragility functions, and probabilities of failure are included in the model. Secondly, a multilayer approach is used to represent various interdependent networks. Finally, the temporal dimension of the problem is considered through a tensor representing the different configurations of the system that are active at each time step. The probabilities of occurrence of different configurations have been calculated considering also temporal effects such as the autonomy of backups.

Compared to the traditional IIM and to fault-tree analysis, the proposed modified IIM offers significant advantages compared to the original one: (i) it can highlight changes in the system's configuration after each node's failure; (ii) the multi-layer representation facilitates the calculation of the cascading failure probability for each node; (iii) probabilities of occurrence (P_{occ}) give straightforward information on the state of each chain and allows the evaluation of temporal effects; (iv) it allows infrastructure managers to identify critical nodes and evaluate possible damages to other networks.

The methodology has been tested on a case study inspired by the events of the 2011 Fukushima Dai-ichi nuclear power plant disaster. Two models have been developed to understand how the complexity of the topology of the system affects the analysis. Interdependencies between the power and water systems and their changes in the aftermath of the disaster have been highlighted. Results showed that the modified IIM is able to represent accurately the sequence of events that occurred in Fukushima even using a simplified model. This is a positive outcome since it means that it is a useful tool that can be used in a preliminary

phase when only little information is available. Compared to other simplified methods used in preliminary analyses, this one crucially accounts for the time component, showing the evolution of the probability of occurrence of various configurations. However, adding more complexity to the topology of the system was beneficial. The detailed model was indeed more reliable and capable of providing a better solution to evaluate the temporal effects. In this model elements of other infrastructures at the regional scale were introduced. This shows that the proposed IIM can be applied at larger scales. Obviously, the definition of all possible network configurations can be a daunting task considering that configurations can also vary depending on the hazard, as different hazards generate different types of damages. In the specific case of nuclear power plants and other critical facilities, this should be easier because possible configurations are known from emergency plans. Depending on the damaged components, certain backup systems would activate based on predetermined plans. The main challenge is represented by the number of nodes that are introduced in the model. Developing the interdependency matrix at node level when the network has hundreds of nodes could be time-consuming. Nonetheless, the presented case study showed that even with limited information it is possible to define a number of possible system configurations and evaluate their probability of occurrence. Moreover, since many of the components and backup elements described in the case study have an equivalent in other systems, the proposed method can be easily extended to other network-like systems. As shown in the detail model example, the modified IIM can also be applied on different scales, from the single system to multi-regional systems, by properly modeling the interdependencies and adding nodes in the topology of the model. Such method could provide valuable information to decision makers for performing loss analyses, increasing preparedness, and devising emergency plans.

Relevance to resilience

The research provides a method for modeling the resilience of complex network-like systems, such as nuclear power plants. The method accounts for both the time component and interdependencies. The work also allows evaluating the failure probability of different system configurations for a more accurate system resilience calculation.

The topic of the manuscript is relevant to resilience because:

1. It deals with the issues of infrastructure interdependencies during disaster. Reducing infrastructure interdependencies will improve resilience of infrastructures toward disasters;
2. The time dimension that is an important aspect of the recovery process after the disaster is taken into account by considering the variability of the interdependency during the disaster;

Declaration of competing interest

The authors declare that they have no known competing financial interests or personal relationships that could have appeared to influence the work reported in this paper.

CRediT authorship contribution statement

Gian Paolo Cimellaro: Conceptualization, Project administration, Supervision, Methodology, Funding acquisition. **Alessandro Cardoni:** Data curation, Validation, Writing – original draft, Writing – review & editing. **Andrei Reinhorn:** Conceptualization, Methodology, Supervision.

Acknowledgments

References

[1] Poljanšek K, Bono F, Gutiérrez E. Seismic risk assessment of interdependent critical infrastructure systems: the case of European gas and electricity networks. Earthq Eng Struct Dyn 2012;41(1):61–79.

[2] Dueñas-Osorio L, Craig JI, Goodno BJ. Seismic response of critical interdependent networks. Earthq Eng Struct Dyn 2007;36(2):285–306.

[3] Cimellaro GP, Solari D, Bruneau M. Physical infrastructure interdependency and regional resilience index after the 2011 Tohoku Earthquake in Japan. Earthq Eng Struct Dyn 2014;43(12):1763–84.

[4] Rinaldi SM, Peerenboom JP, Kelly TK. Identifying, understanding, and analyzing critical infrastructure interdependencies. IEEE Control Syst Mag 2001;21(6):11–25.

[5] Zimmerman R. Social implications of infrastructure network interactions. J Urban Technol 2001;8(3):97–119.

[6] Dudenhoeffer DD, Permann MR, Manic M. CIMS: a framework for infrastructure interdependency modeling and analysis. In: Proceedings of the 38th conference on winter simulation, winter simulation conference; 2006. p. 478–85.

[7] Lee EE II, Mitchell JE, Wallace WA. Restoration of services in interdependent infrastructure systems: a network flows approach. IEEE Trans Syst, Man, Cybern, Part C (Appl Rev) 2007;37(6):1303–17.

[8] Zhang P, Peeta S. A generalized modeling framework to analyze interdependencies among infrastructure systems. Transp Res Part B 2011;45(3):553–79.

[9] Cimellaro GP. Urban resilience for emergency response and recovery. Fundamental Concepts and Applications; 2016.

[10] Ouyang M. Review on modeling and simulation of interdependent critical infrastructure systems. Reliab Eng Syst Saf 2014;121:43–60.

[11] Sharma N, Nocera F, Gardoni P. Classification and mathematical modeling of infrastructure interdependencies. Sustain Resilient Infrastruct 2021;6(1–2):4–25.

[12] Haggag M, Ezzeldin M, El-Dakhakhni W, Hassini E. Resilient cities critical infrastructure interdependence: a meta-research. Sustain Resilient Infrastruct 2022;7(4):291–312.

[13] Wang F, Magoua JJ, Li N. Modeling cascading failure of interdependent critical infrastructure systems using HLA-based co-simulation. Autom Constr 2022;133:104008.

[14] Hossain NUI, El Amrani S, Jaradat R, Marufuzzaman M, Buchanan R, Rinaudo C, Hamilton M. Modeling and assessing interdependencies between critical infrastructures using Bayesian network: a case study of inland waterway port and surrounding supply chain network. Reliab Eng Syst Saf 2020;198:106898.

[15] Tang P, Xia Q, Wang Y. Addressing cascading effects of earthquakes in urban areas from network perspective to improve disaster mitigation. Int J Disaster Risk Reduct 2019;35:101065.

[16] Bigger JE, Willingham MG, Krimgold F, Mili L. Consequences of critical infrastructure interdependencies: lessons from the 2004 hurricane season in Florida. Int J Crit Infrastruct 2009;5(3):199.

[17] Yang Y, Ng ST, Zhou S, Xu FJ, Li H. A physics-based framework for analyzing the resilience of interdependent civil infrastructure systems: a climatic extreme event case in Hong Kong. Sustain Cities Soc 2019;47:101485.

[18] Nan C, Sansavini G. A quantitative method for assessing resilience of interdependent infrastructures. Reliab Eng Syst Saf 2017;157:35–53.

[19] Goldbeck N, Angeloudis P, Ochieng WY. Resilience assessment for interdependent urban infrastructure systems using dynamic network flow models. Reliab Eng Syst Saf 2019;188:62–79.

[20] Haimes YY, Horowitz BM, Lambert JH, Santos JR, Lian C, Crowther KG. Inoperability input-output model for interdependent infrastructure sectors. I: theory and methodology. J Infrastruct Syst 2005;11(2):67–79.

[21] Avelino AF, Dall'erba S. Comparing the economic impact of natural disasters generated by different input–output models: an application to the 2007 Chehalis river flood (wa). Risk Anal 2019;39(1):85–104.

[22] Tamssaouet F, Nguyen KT, Medjaher K. System-level prognostics under mission profile effects using inoperability input–output model. IEEE Trans Syst, Man, Cybern 2019;51(8):4659–69.

[23] Garcia-Hernandez JA, Brouwer R. A multiregional input–output optimization model to assess impacts of water supply disruptions under climate change on the Great Lakes economy. Econ Syst Res 2021;33(4):509–35.

[24] Huang R, Malik A, Lenzen M, Jin Y, Wang Y, Faturay F, Zhu Z. Supply-chain impacts of Sichuan earthquake: a case study using disaster input–output analysis. Nat Hazards 2022; 110:2227–48.

[25] Setola R, Oliva G, Conte F. Time-varying input-output inoperability model. J Infrastruct Syst 2012;19(1):47–57.

[26] Santos JR, Yu KDS, Pagsuyoin SAT, Tan RR. Time-varying disaster recovery model for interdependent economic systems using hybrid input–output and event tree analysis. Eco Syst Res 2014;26(1):60–80.

[27] Niknejad A, Petrovic D. A fuzzy dynamic inoperability input–output model for strategic risk management in global production networks. Int J Prod Econ 2016;179:44–58.

[28] Holme P, Saramäki J. Temporal networks. Phys Rep 2012;519(3):97–125.

[29] Sun W, Bocchini P, Davison BD. Overview of interdependency models of critical infrastructure for resilience assessment. Nat Hazards Rev 2022;23(1):04021058.

[30] Elkmann P. Emergency planning for nuclear power plants. CRC Press; 2017.

[31] Wall IB, Haugh JJ, Worlege DH. Recent applications of PSA for managing nuclear power plant safety. Prog Nucl Energy 2001;39(3–4):367–425.

[32] He X, Tong J, Chen J. Maintenance risk management in Daya Bay nuclear power plant: PSA model, tools and applications. Prog Nucl Energy 2007;49(1):103–12.

[33] U. NRC, Issuance Of Order To Modify Licenses With Regard To Requirements For Mitigation Strategies For Beyond-Design-Basis External Events, Washington, DC (2012).

[34] Gjorgiev B, Volkanovski A, Sansavini G. Improving nuclear power plant safety through independent water storage systems. Nucl Eng Des 2017;323:8–15.

[35] Valencia VV, Thal AE, Colombi JM, Sitzabee WE. Infrastructure decay modeling with the input-output inoperability model. ASCE-ASME J Risk Uncertain Eng Syst, Part B 2015;1(1):011006.

[36] Leontief W. Input-output economics. Oxford University Press; 1986.

[37] Rojahn C, Sharpe RL. Earthquake damage evaluation data for California. Applied Technology Council; 1985.

[38] Eidinger J, Avila E, Ballantyne D, Cheng L, Der Kiureghian A, Maison B, O'Rourke T, Power M. Seismic fragility formulations for water systems. Reston, VA: American Lifelines Alliance; 2001.

[39] FEMA Hazus-MH 2.1 technical manual. Washington, DC: FEMA; 2013.

[40] Moriya K, Sato K. Fukushima Daiichi NPP accident: plant design and preliminary observations. Int. congress advances in nuclear power plants (ICAPP 2011) Nice, France; 2011.